

**ISTC Project No. G-2188**

**Investigation into visualization of prostate cancer at early stage of  
development**

**Final Project Technical Report**

**on the work performed from March 01.2016 to March 01.2018**

**Tbilisi State Medical University**

**Project Manager      Alexandre khuskivadze  
MD, PhD**

\_\_\_\_\_

**Director                Zurab Vadachkoria  
MD, PhD**

\_\_\_\_\_

\_\_\_\_\_

Title of the Project: **Investigation into visualization of prostate cancer at early stage of development**

Commencement Date: 01.03.2018

Duration: 24 months

Project Manager Alexandre Khuskivadze

phone number: (995) 593 313 015

fax number: n/a

e-mail address: a\_khuskivadze@yaahoo.com

Leading Institute: Tbilisi State Medical University  
3, Vazha-Pshavela awe. Tbilisi, Georgia  
995 32 542445  
Pr@tsmu.edu  
<https://tsmu.edu/tsmu2/>

Participating Institutes: <Name>  
<Address>  
<Phone>  
<Email>  
<URL> if exist

Foreign Collaborators: Jeffrey Karnes  
USA, Rochester, 200 First street WS  
7 449 9780110  
Karnes.R@mayo.cdu

Foreign Collaborators: Henri Lai  
USA, Seattle, University of Washington, Box355061  
(I )(206) 5431071  
hlai@u.washington.cdu

Keywords: prostate, cancer, infrared, image, radiation

**LIST OF CONTENTS**

1. Brief description of the work plan: objective, expected results, technical approach .....	4
2. Method, Experiments, Theory etc. ....	5
3. Results .....	11
4. Conclusion.....	39
5. References .....	39

## 1. Brief description of the work plan: objective, expected results, technical approach

Prostate cancer is very common disease among men. After the lung cancer it has second place as a cause of morbidity worldwide. Prostate cancer has no symptoms for a long time and it makes early diagnosis harder to determine. Screening tests can help us to fight the cancer. That's why we make PSA analysis at first. Normal ratio is below 4ng/ml in blood. If PSA levels rises more then 10 ng/ml, the chance of cancer increases. By the way, PSA is prostate cancer specific marker, its elevation may be caused by other factors too. For example: inflammatory processes, BPH, trauma and e.t.c after obtaining PSA levels doctors continue other diagnostic procedures. Digital rectal examination: where we can feel nodes of prostatic tissue and its texture. There are other diagnostic imaging tests too, for example magnetic resonance imaging (MRI). MRI uses strong magnetic field and high frequency electro-magnetic waves. This information is delivered and transformed in computer into MRI image. MRI side effects are its invasiveness- strong magnetic field (1-5 tesla). also we cannot always diagnose small sized cancerous nodes. There is new technology - intra rectal MRI, but this method is new and not fully developed. The next imaging diagnostic tool is positron embossing tomography (PET). this method gives us 3 dimensional image on CT scan. The radio nucleotide concentration of cancerous tissue differs from the normal one. The bad side of this diagnostic test is its difficulty, needing high skilled radiologist and doctor. PET is partly invasive because of X and gamma rays. The rectal ultrasaound is not invasive, but we do not use it for prostate cancer diagnosis. It has role in doing biopsy procedure. The last word for prostate cancer diagnosis goes to biopsy, because any listed imaging studies are verified by biopsy and pathological results of it. Unfortunately biopsy is not as easy to do. there are guidelines which give us strict rules, how we should take specimans ( we take 12 specimens from both side of prostate gland). If the cancer is too small primary biopsy could not catch it. The needle may be aimed to normal tissue. misunderstanding occurs for these patients, because PSA and other diagnostic tests show the cancer, but the biopsy is negative. In this situation new biopsy is needed. There were cases that only after 5<sup>th</sup> biopsy the patient was diagnosed to have prostate cancer. The side effect of biopsy is spread of cancerous cells in bloodstream, which may cause metastasis.

That's why early diagnosis of prostate cancer is quite difficult. This is the reason why more than 6 million people are dying yearly worldwide from the prostate cancer. This was the main reason why we started to make this project. Our wish was to have new diagnostic tool for prostate cancer early diagnosis.

For achievement of main objective following tasks were plnned:

1. Investigation of the noncancerous and cancerous prostate tissues in the IR light. This conceived patients' surgical operations during of all project implementation.
2. Investigation of IR light penetration in prostate tissue in passed mode. This task consisted from 4 subtasks:
3. a) Investigation IR light penetration dependence on IR light wavelength; b) Investigation IR light penetration dependence on tissue thickness. c) Investigation of IR images of the noncancerous prostate tissues and d)

Investigation of IR images of the cancerous prostate tissues.

4. Investigation of prostate IR images in back scattered mode.
5. Investigation of the prostate IR images in the polarized IR light in passed mode.
6. Development and preparing of working model of device for prostate cancer diagnosis,
7. Development of Software of processing of prostate IR images.

Expected result in accordance with the stages of development were

: **Obtaining of new knowledge concerning:**

- Penetration of IR light in noncancerous prostate tissue for passed mode.
- Penetration of IR light through prostate cancerous tissues in passed mode.
- Reflection of IR light through prostate cancerous tissues in back scattered mode.
- Optical properties of the prostate tissue in the polarized IR light.
- Development of software for computer analysis and processing of the prostate tissue IR images.
- Development of the working model of the device for prostate cancer early detection.

A final diagnosis device would imply: IR light source- small IR LED- or thin optic fiber placed through urethra at the center of prostate. Infrared LEDs existing at market are small enough and of different power. They had to be placed in flexible catheters. Catheter had to easy slip to prostate. Illumination of prostate with IR light was possible also in another way: Side glow fiber optic wisp with small diameter would be slipped into the prostate through urethra. Another end of the fiber optic with head illuminated with IR light. It is possible another scenario for prostate illumination: an infrared light source had to be placed at the lower part of the abdomen. Infrared light passes through all tissues and the prostate gland. The CCD camera placed in the rectum will receive information about gland malignancy.

Concerning obtaining of prostate IR images- High resolution IR CCD camera was necessary, which would be placed in the rectum. It is possible to manufacture CCD camera with dimension not exceeding 10 mm. Such camera with all schemes and wires might be mounted on the probe. Output of CCD camera will be connected to the PC via USB port. Doctor will scan prostate with probe, like digital examination. The monitor will be divided into two parts. On one of them IR images will be shown in online mode. The other half of the monitor will show the image processed by the software. This image will be reflected in various colors, some of such colors will be indicative of the cancer formation.

## 2. Method, Experiments, Theory etc.

Experimental methods.

On the figure 1 is shown experimental block scheme, by which we can learn how infrared lights pass through prostate tissue according to wave length and tissue thickness.

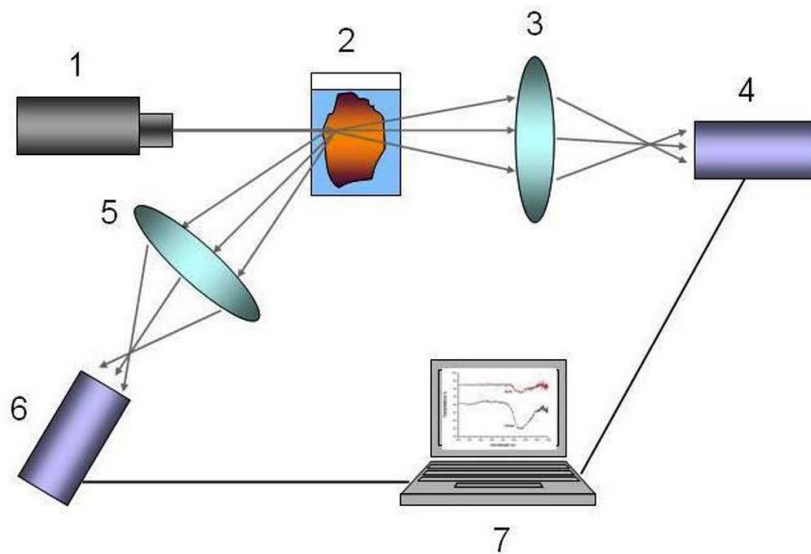


*figure 1. Content: 1-infrared light origin ; 2- prostate tissue slice, 3 and 5- lens system, 4 - 6 spectrophotometer, 7- computer.*

The scheme enables us to study not only penetrating infrared light through prostate (in this case light beam travels through the lens 3 and goes to spectrophotometer 4), but also reflected light from prostate tissue in this case light beam travels through the lens 5 and goes to spectrophotometer 6).

The experiments were carried out using “AVANTES” spectrophotometer. Figure 2 - Experimental model. Information from spectrophotometer is transferred to computer, where it's processed by AVANTES program.

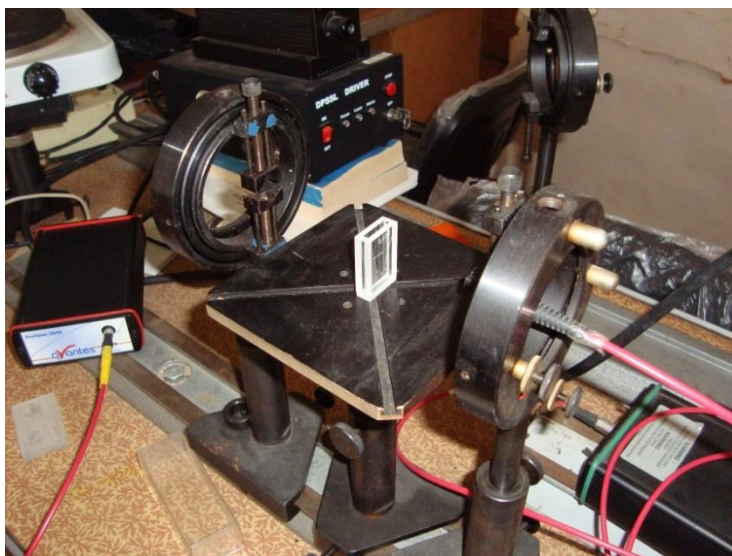


*figure 2. Specimen with prostate tissue is placed on the examination table. The cuvette ensures prostate tissue constant thickness. The wavelength of the IR lights pass through the tissue is 700-1100nm. The*

*spectrophotometer is connected with computer and its program (avantes software), where information is gathered and analyzed.*

The prostate tissues were obtained during trans urethral resection, prostatectomy (in the case of diagnosis of BPH) and radical prostatectomy (in the case of diagnosis of prostate cancer) operations. Tissues were sliced and placed in cuvette.

The bloc scheme of taking prostate infrared images is shown in the figure 3.

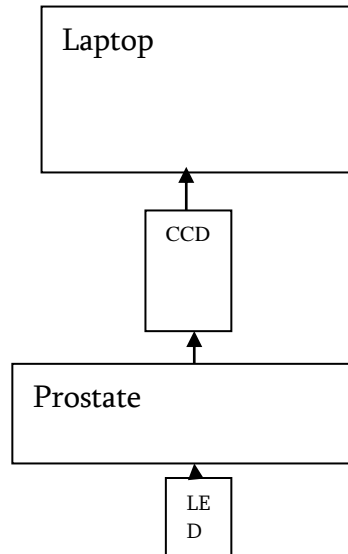


*Figure 3. bloc scheme : IR rays from light emitting diode (LED) transmit through the prostate and enter CCD camera, signals from CCD camera enter into laptop, where IR image is formed.*

On figure 4 is shown prostate IR investigation device. In the frame of the project we purchased CCD camera "IR 1000". IR light source LED and CCD camera are placed on the microscope frame.

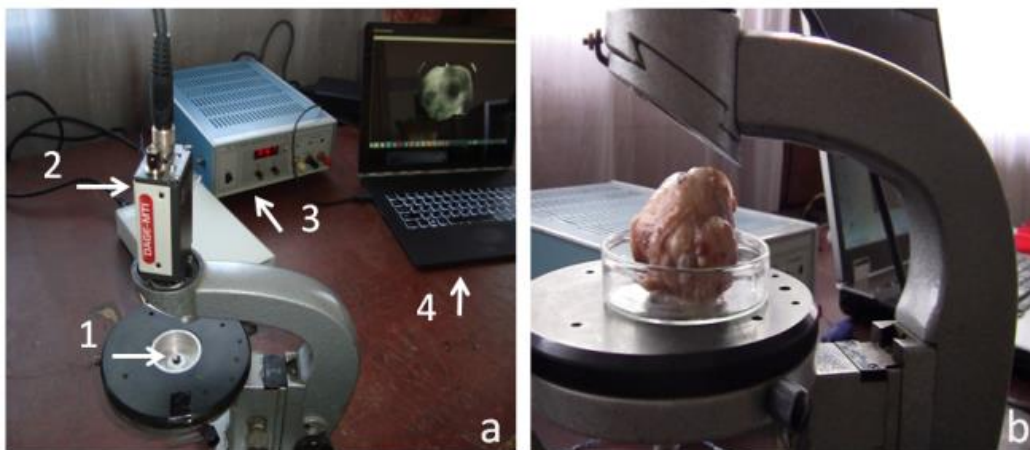


*Figure 4. Experimental setup.*

In figure 4a, arrows 1, 2, 3, and 4 indicates LED, CCD camera, power supply for LED, and laptop, respectively. Figure 4b shows a prostate gland placed on a Petri dish between the CCD camera and LED. NIR light irradiation angle of LED was  $90^\circ$ . The CCD camera capture area covered the whole surface of the prostate gland exposed to NIR, thereby, no scanning was necessary.

Different wavelength, irradiation angle and intensity IR light LEDs were used for prostate illumination. We also used IR laser. On the figure 5 are shown part of used LEDs and IR laser.

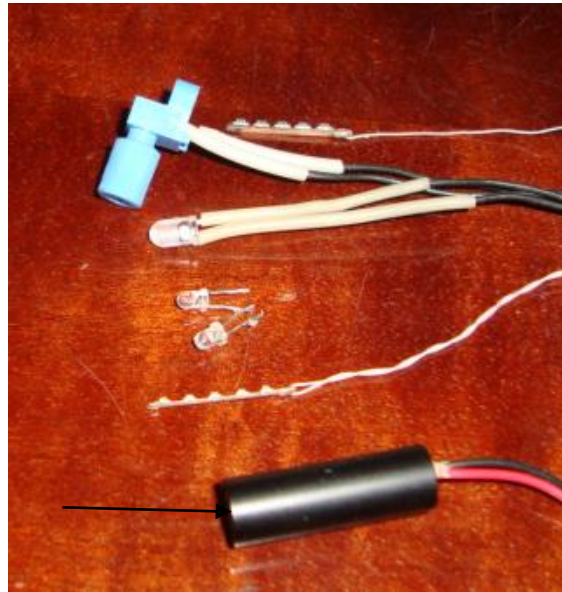


*Figure 5. The part of LEDs and laser used in experiment (Shown with arrows).*

The LEDs were used either placing them into urethral channel of the prostate, or outside the prostate gland. In first case IR lights pass through the peripheral zone of prostate, in second-through the whole prostatic tissue.

On figure 6 is shown another lighter, which we used when prostate was too big in size and photodiode with small strength could not be used to get IR images.

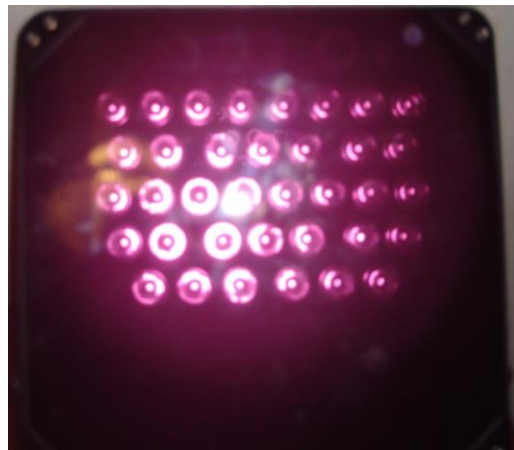
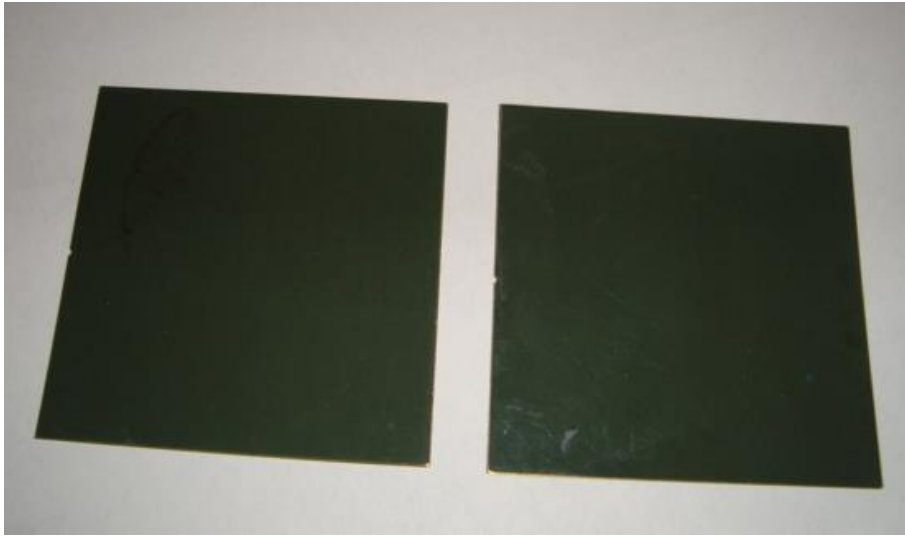


Figure 6. IR lighter. Big sized prostate is placed on petri dish and then placed above infrared lighter.



The project included investigation with polarized light rays. That's why we have purchased polarized filters (APIR29-030 U.S.A, 700-2000 nm) –Figure 7.



*Figure 7. Polarized filters type APIR29-030*

Infrared light passes through CCD camera lens and then falls on CCD camera active matrix, where it is transformed into electrical signals (this is like the process of light passing through retina, which is then converted into neuronal impulses). The CCD camera is connected to a laptop, where developed computer program converts signals into the images; this is the way IR images are formed.

In real situation prostate tissue illumination with IR rays conceives two scenarios. At first case, which will be less disturbing for the patient, the IR light source is placed on the abdomen (tightly) and the CCD camera is placed in the rectum, closer to the prostate gland. So IR rays pass through the prostate tissue and enter the CCD camera. At second case, the IR light source is placed in the prostatic urethra; the scheme is shown in Figure 8.

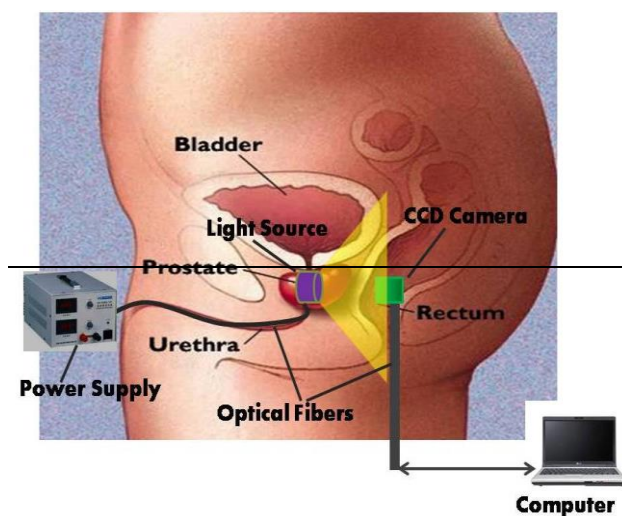


*Figure 8. The prostate lighting scheme with IR rays. IR light source –LED or optical fiber will be placed in urethra. CCD camera will be placed in the rectum.*

On the next figure is shown side glow optics fiber, which was used in experiment to light up prostate tissue from urethra.



*figure 9. Side glow optics fiber. The optic fiber will be placed in the urethral channel. Infrared light source is attached at the end of the optical fiber, which allows to produce side light on whole length. This light is transferred to CCD camera (the infrared light is invisible for human eyes).*

histo-morphological methods: after radical prostatectomy the gland is weighted, sized in three projections, with 4 mm right angle dissector perpendicular to urethra, incisions are made. Each slice is cut into four parts and numerated right, left, anterior and posterior parts. Sectional slices are placed on cassettes for further preparation. Each slice is documented with photo. After pouring paraffin each block is cut with microtome into 4 mm slices. Then it is dyed with hematoxilin-eosin dye. The microscopic investigation: to determine morphological state surgical margins (apex, prostate base, left and right side) are explored. Then we should determine exact location of malignant tissue. After this we determine histological type and Gleason score, which helps us to determine stage of malignant cancer. Also we determine its patten (primary, or secondary tumor); volume of malignant tissue, size of malignant tissue in mm, pathological stage (pTNM); capsular integrity, invasiveness in seminal vesicles and metastasis in lymph nodes; also perineural and perivascular invasiveness are determined.

On the figure 10 it is shown prostate gland processed this way.



*Figure 10. prostate gland processed in formalin and ready for histo-norphological analyzes.*

### 3. Results

#### Results discussion:

In order to achieve the final goal, a number of tasks that would have been accomplished.

One of the first tasks was to study prostate tissue dependence from the wave length of the spectrum infrared range. Experiments showed that visible light does not pass through prostate tissue. Only infrared lights passes through this tissue. Besides, infrared light transition depends on the infrared light wavelength. Experiments have shown that highest transparency was for 840-860 nm wavelength. It was shown that normal and pathological tissues have different transparent potential. The highest transparency has normal tissue; the transparency of malignant tissue is much lower. The transparency of benign prostate hyperplasia (BPH) tissue is between the normal and cancerous tissues. On the figure 12 is shown results of this investigation.

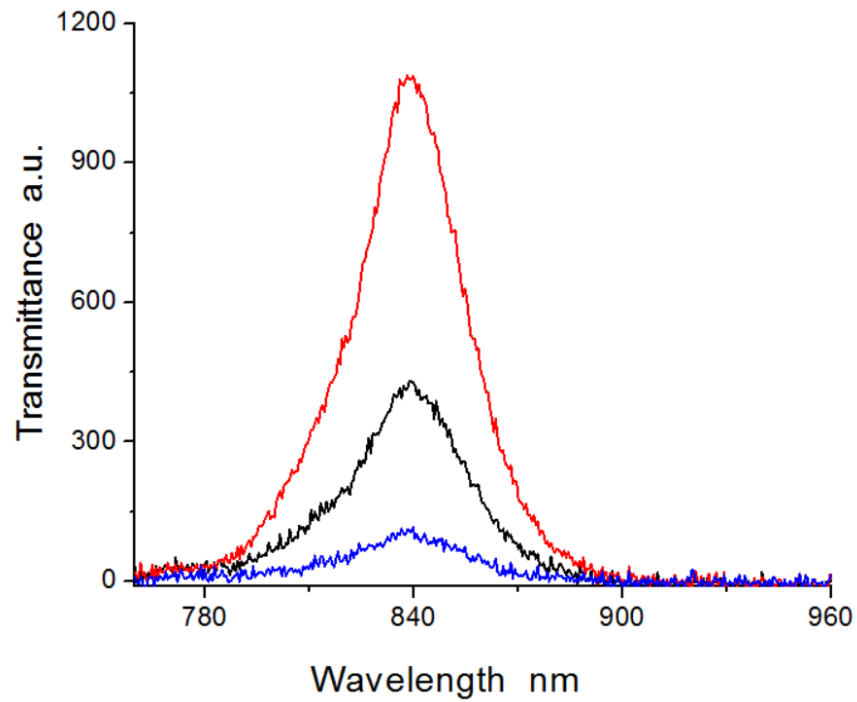


*Figure 12. Transparency of prostate tissue with different thickness depends on different wavelength IR light. The red graphic shows transmittance of normal tissue depended on wavelength. Maximum transmittance value is 1100 A.U. The blue graphic shows transmittance of cancerous tissue- max. value is 140 A.U. The dark green graphic shows BPH tissue transmittance- max. value is 480 A.U. The X-axis shows wavelength , Y-axis shows transmittance in A.U.*

Experiments revealed, that maximal transmittance for these three tissues has same wavelength- 840 nm.

In other series of experiments IR light transmittance in different thickness tissues and their relationship was studied. Experiments showed that IR light transmittance depends on prostate tissue thickness. The more thickness tissue has, the less transparent it is and vice versa. On the figure 13 is shown normal prostate tissue transparence depended on thickness.

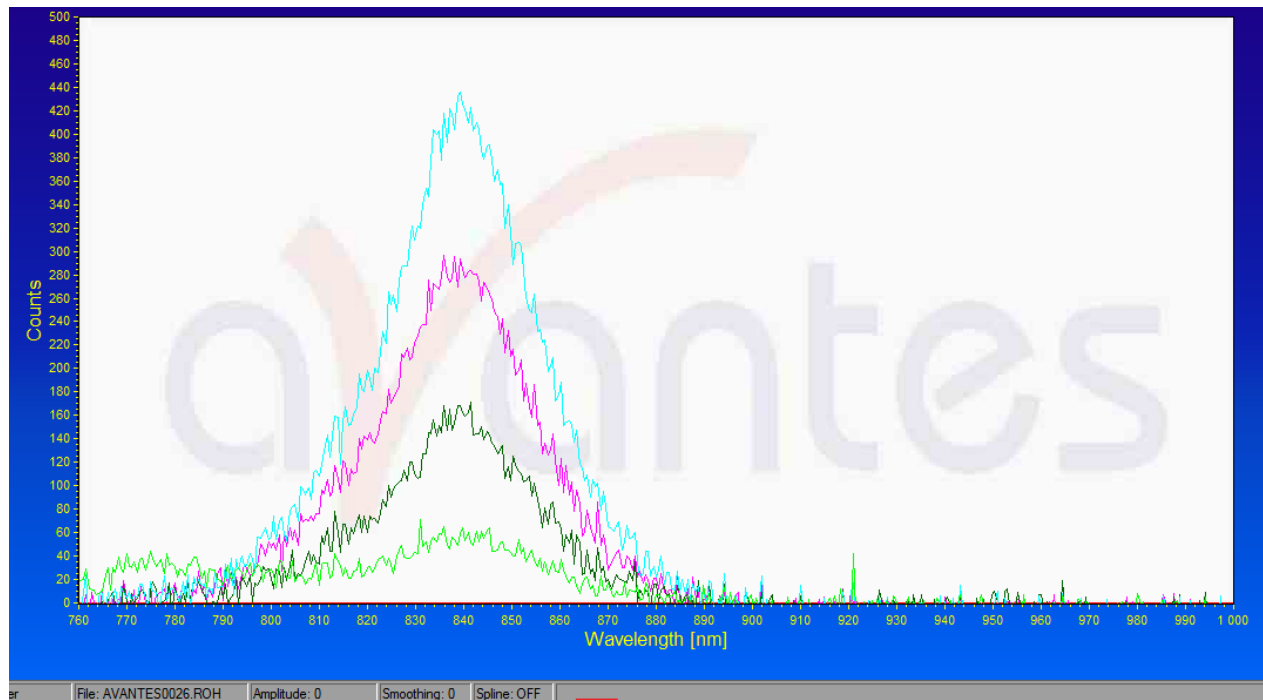


*Figure 13. transparency of normal prostate tissue depended on different thickness. The light blue graphic is for 2 mm thick tissue, the purple -6mm, dark green-8mm, and light green 15mm. The max. transmittances are 435 A.U, 160 A.U and 50 A.U.*

Experiments showed that, in nonmalignant tissue highest transmittance relationship with tissue thickness has linear structure. Obtained relationship for prostate tissues with benign prostatic hyperplasia was similar to this – figure 14.

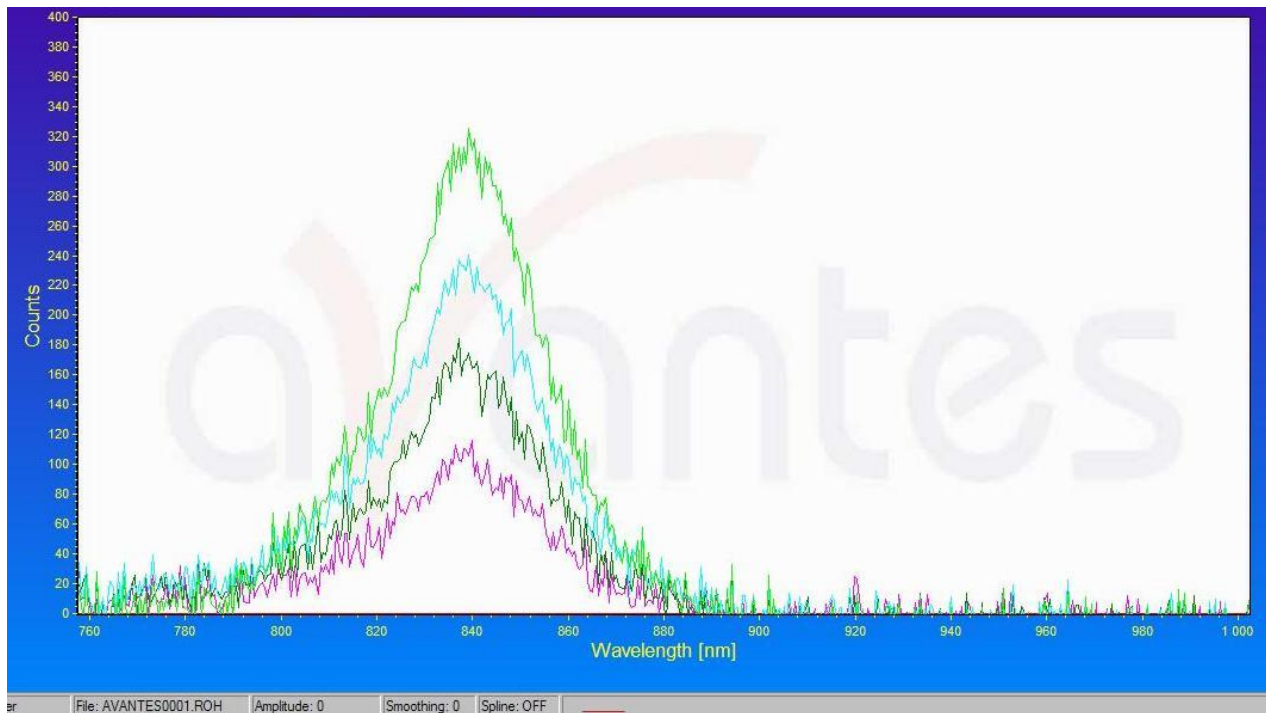


*Figure 14. Different transmittances according to tissue thickness. Graphic shows us prostate tissues with benign prostatic hyperplasia. The light green graphic is of 5mm thick tissue, with max. Transmittance 320 A.U, Light blue graphic -10mm, with max. transmittance 220 A.U., The dark green- 15 mm, maxes. transmittance-170 A.U., The purple – 20 mm, max. transmittance 100 A.U. Wavelength for all maximal transmittance is 840 nm. X- axis corresponds to wavelength in nm, Y-axis corresponds to transmittance in A.U.*

The maximal value for transmittance according to different tissue thickness is linear, like in a healthy tissue. Experiments have shown that this relationship for the malignant (cancerous) tissue it's not the same. On the figure15 is shown cancerous tissue transparency according to tissue thickness.

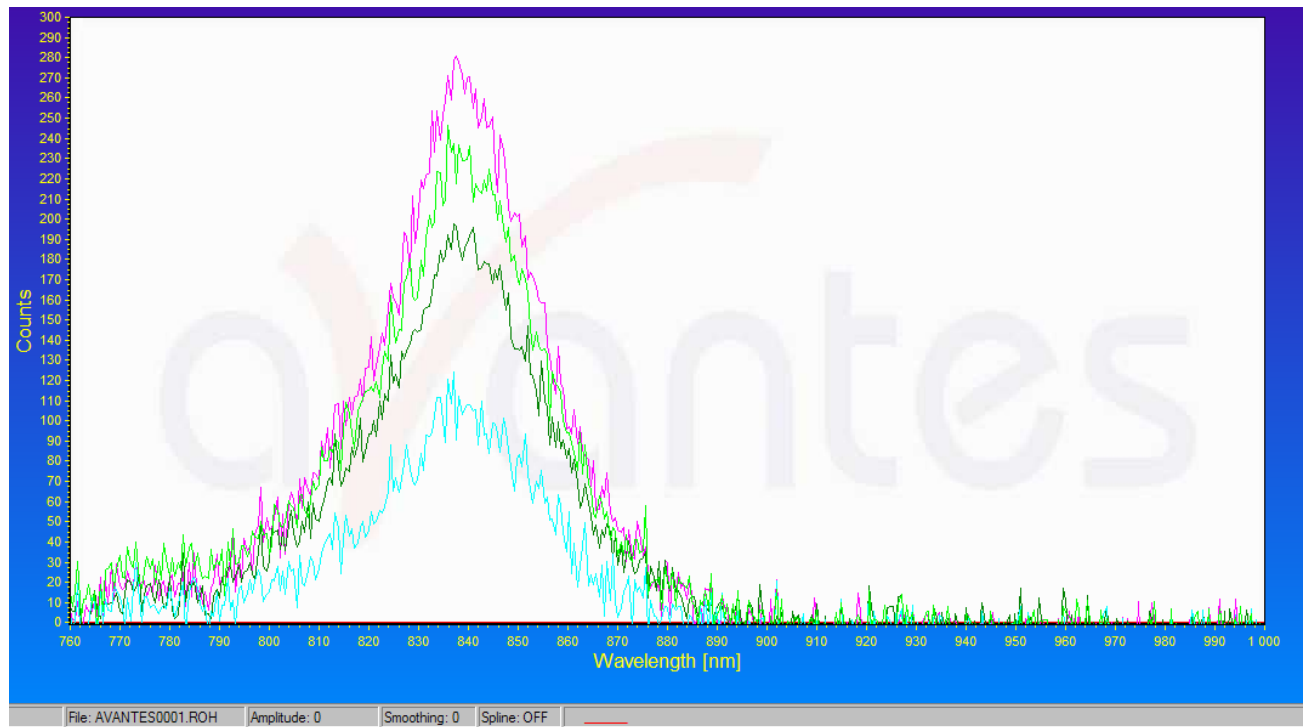


*figure 15. Transparency and tissue thickness relationship in prostate cancer patients. The purple graphic is for 2 mm thick tissue, light green for-4 mm, dark green for -6mm, light blue- 10 mm. The maximal transmittance for each curve is 280 A.U, 185 A.U and 90 A.U.*

In our experiments the transmittance dependence on IR light intensity was also studied. For this reason, we used different power light sources, but IR wavelength and tissue thickness stayed constant. On the figure 16 is shown transmittance dependence on wavelength and intensity.

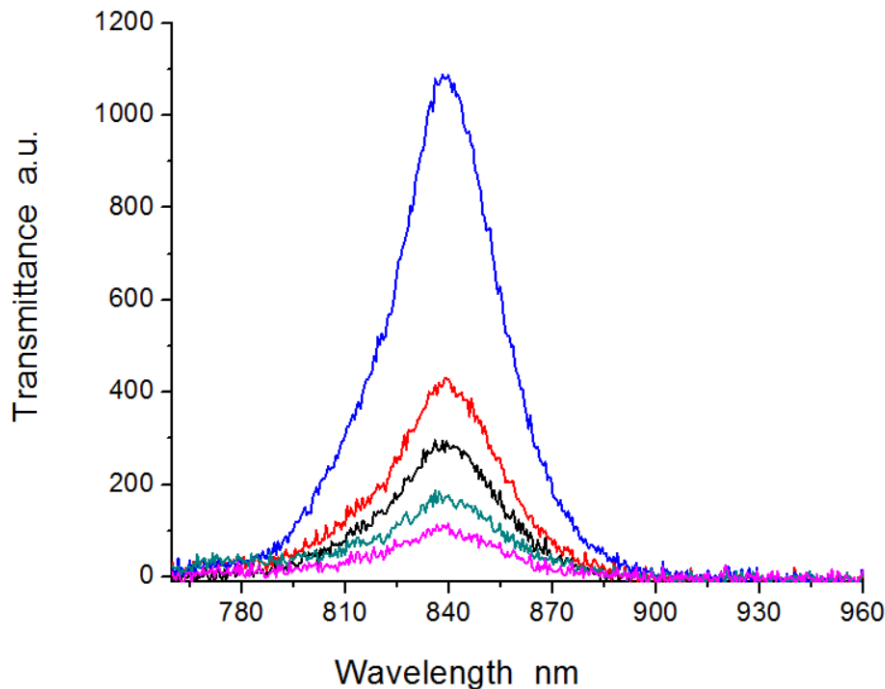


*Figure 16. transmittance dependence on wavelength and intensity. For all case maximal transmittance is at the wavelength equal to 840 nm. The blue graphics shows maximal intensity 160 mW/steradian, the red - 35 mW/steradian, the dark green shows 25 mW/steradian, light green - 10 mW/steradian and purple - 4 mW/steradian.*

Thus, experiments have shown that IR light has good transmittance through the prostate tissue. Maximal transmittance is 840-860 nm. The cancerous, nonmalignant and normal tissues have different transmittances: The highest transmittance has normal tissue, while the cancerous one has the lowest. Transmittance can be regulated by controlling of the emitted light intensity. The relationship of transmittance and tissue thickness in normal tissue is linear, while it is nonlinear in cancerous case.

The different surgical operations were made because of different diagnosis. For example, radical prostatectomy was done because of prostate cancer, transvesical prostatectomy was performed for BPH and for urine continence - TUR(P)s. After every operation prostate tissue was examined with IR lights.

The IR light passes through prostate and enters CCD camera, which is connected to the computer. Illumination of the prostate is important for getting IR image and working on it. That's why; we studied how different light has effected on getting IR images. In the experiments we used different intensity LEDs with different angles of irradiation. When irradiation power is same, irradiated energy concentration is more in LED which has lesser angle of irradiation and vice versa. Because of these, optimal IR image is taken with wide angle LED. On the figure 7 the same prostate IR images are taken with different angle photodiodes.





*Figure 17. figure on the left- Nonmalignant prostate tissue IR image taken with  $15^\circ$  irradiation angle LED. Figure on the right - The same prostate image taken with  $45^\circ$  irradiation angle LED. Here we can conclude that wide angle LED can visualize whole prostate tissue, whereas narrow angle photodiode enables only partial visualization. At the end of the figure 1 cm is shown for scale.*

LED, which has wide irradiation angle (approximately  $150^\circ$ ), can visualize surrounded areas of prostate gland too. The experiments showed that optimal LEDs have irradiation angle with  $90^\circ$ . We concluded that quality of IR image depends on photodiode energy strength. Optimal energy enables us take good quality images of prostate, which is illustrated on figure 18.

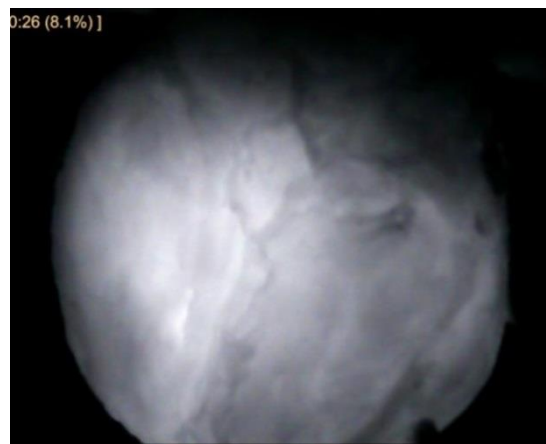


*Figure 18. IR image of the prostate. The LED irradiated energy is 90 mWat/steradian, the irradiation angle is equal to  $90^\circ$ . The image is irradiated from rectum side.*

If energy irradiated from the LED is less than optimal, it enables us to visualize only part of the image-figure 19.

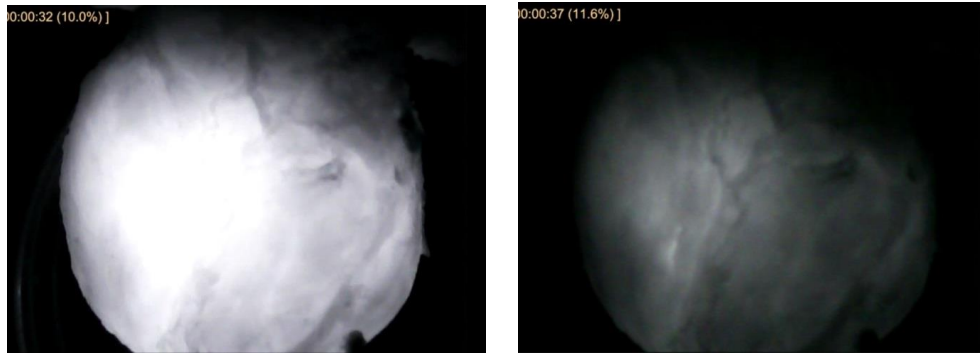


*Figure 19. Nonmalignant prostate IR images taken with different power LEDs. On the left- we see prostate IR image, which is illuminated 130 mW/steradian strength LED. On the right- The prostate image is taken with 30 mW/steradian LED.*

When IR photon enters prostate tissue, it scatters. The parts of photons are absorbed by the tissue and part passes through it. That's why prostate IR image brightness depends on tissue thickness i.e. on prostate size. The less is prostate tissue thickness the more surface is exposed to CCD camera and vice versa. So IR illumination depends on the length of the path that photon passes; the less the length is, the more is image brightness, because there is less probability of photon absorption. If thickness of prostate is constant the image is homogenous. The lighting of prostate tissue according to its thickness is shown on the figure 20.

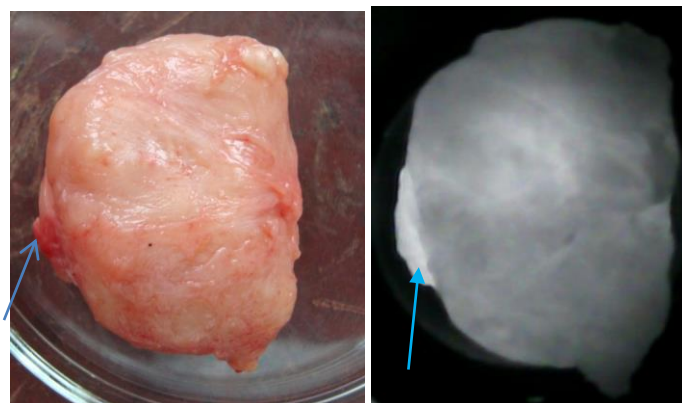


*Figure 20. The IR image of prostate tissue with different thickness (nonmalignant prostate). On the left figure is shown prostate photography. On the right is shown prostate IR image. The image has homogenous brightness. Exceptions is parts shown with arrows. It is easily identify that, prostate thickness is less in that areas.*

On the next figure is shown homogenous IR image, which is from BPH patient.

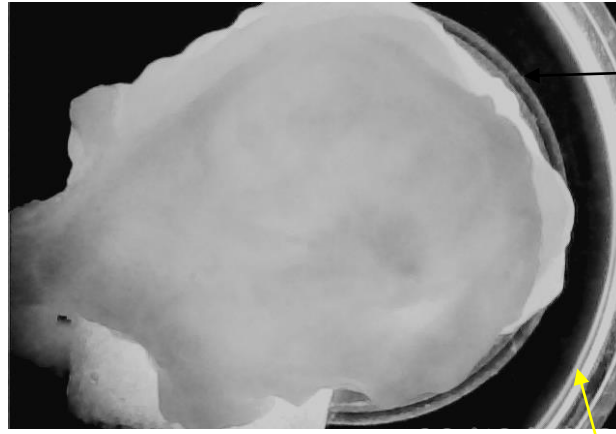


*Figure 21. Infrared image of prostate with BPH. Brighthness of the image is homogenous. The arrows show petry dish margins.*

After IR imaging each prostate tissue was examined histo-morphologically. We processed a prostate in formalin and examine under microscope. This enables us to determine maligncy of the tissue and it's degree. On the figure 22 is shown prostate tissue histo-morphology structure.

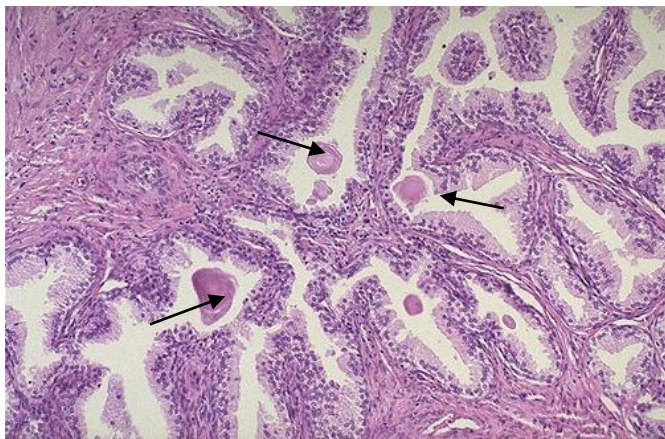


*Figure 22. BPH histo-morphology image. The tissue is well differentiated, we can see stroma and thickened glandular lumen shown with arrows.*

Some experiments were performed after transurethral resection of prostate. On the figure 23 is sown one of this tissues and its IR image. These tissue was nonmalignant.



*Figure 23. On the left- prostate tissue photography after transurethral resection. On the right- Its infrared image. The brightness intensity is homogenous.*

To achieve main goal of the project - the prostate cancer visualization - we needed to examine malignant prostates and analyze their IR images.

Experiments showed that, cancerous prostate IR images differ from nonmalignant ones. The image has different appearance in case of different aggressiveness of the tumor. On the figure 24 is shown cancerous prostate and its IR image. In this case cancer has come out the capsule. On the IR images cancerous area has high optical density.

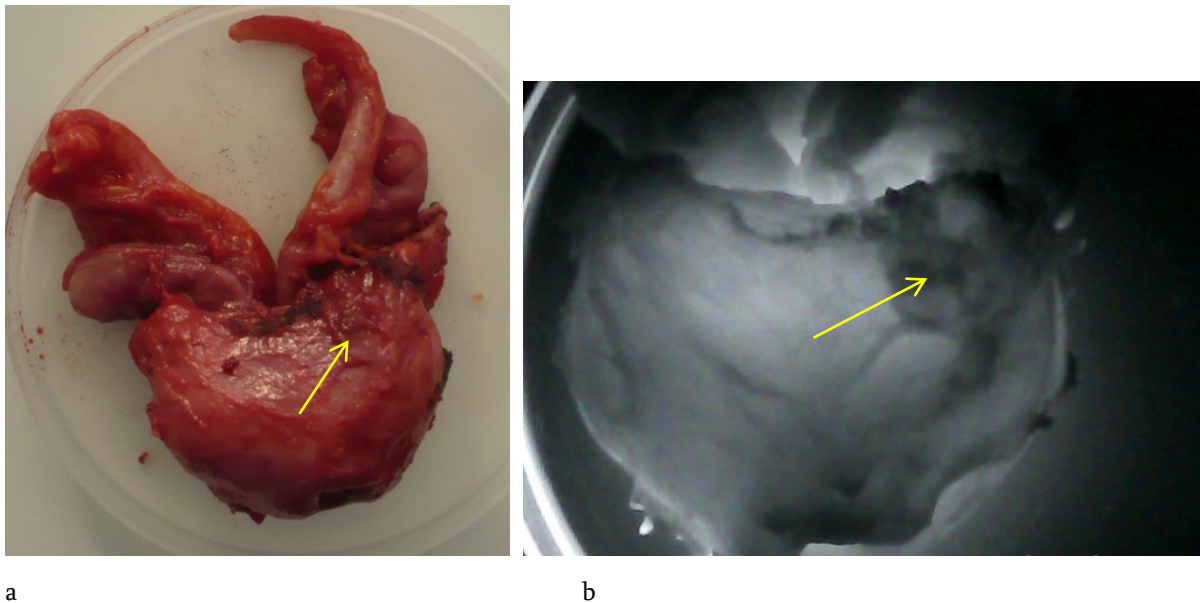


*Figure 24. a) Cancerous prostate photography. b) IR image of this prostate. On the photography and on the IR image malignant tissues are shown with arrow. Both images are taken from rectum side.*



After this IR examination this prostate was investigated histo-morphologically - figure 25.

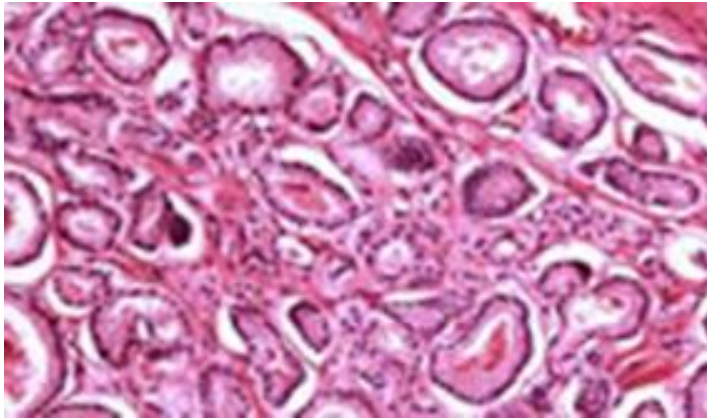


*Figure 25. Prostate cancer histo-morphology image. The cancer has different sized acinuses , which are demonstrated in this picture.*

If cancer doesn't come out prostate capsule, we can not see it on photography. On the figure 26 is shown photography and IR image of one of such prostates. On the photography cancer is not seen, because it doesn't comes out the capsule. On the right figure we see IR image of this prostate. There are dark, high optical density areas, which are shown with arrows.

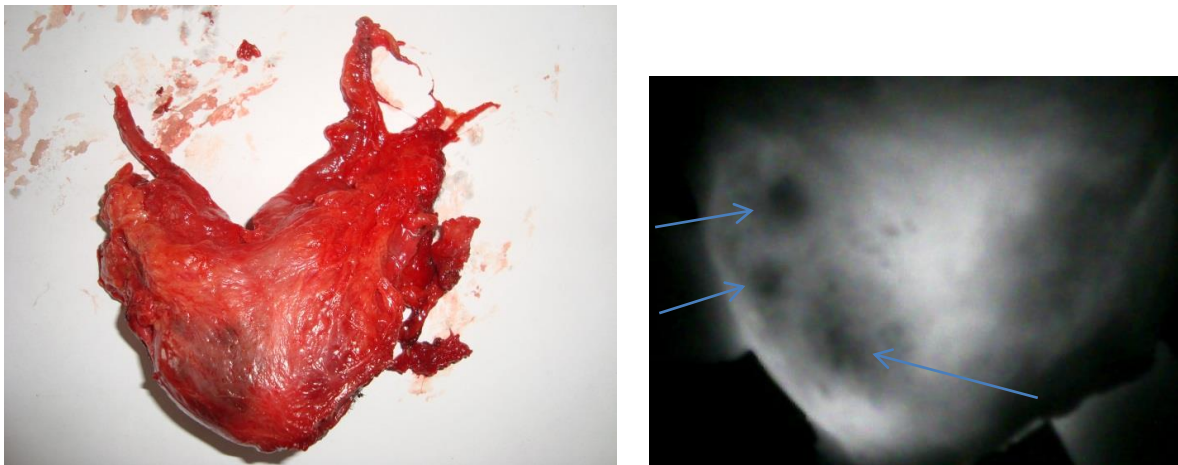


*Figure 26. Left figure -prostate photo. Right figure IR image of the prostate. Malignant areas are shown with arrows.*

Results of histo-morphological investigation of mentioned prostate is shown on figure 27.

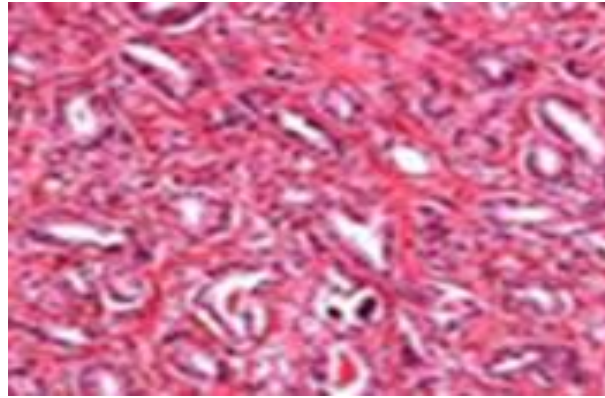


*Figure 27. The malignant areas are composed of complex network, which is attached to urethral structures. Stromal invasion is not seen.*

The prostate cancer has different spectrum of aggressiveness, which are determined by the Gleason score. Above the 5<sup>th</sup> grade the tumor progression is very rapid; it has high chance to penetrate the capsule and metastatic migration.

We examined different prostates with different aggressive pattern malignant tissues.

On the figure 28 we can see two cancerous prostates with different pattern of aggressiveness.

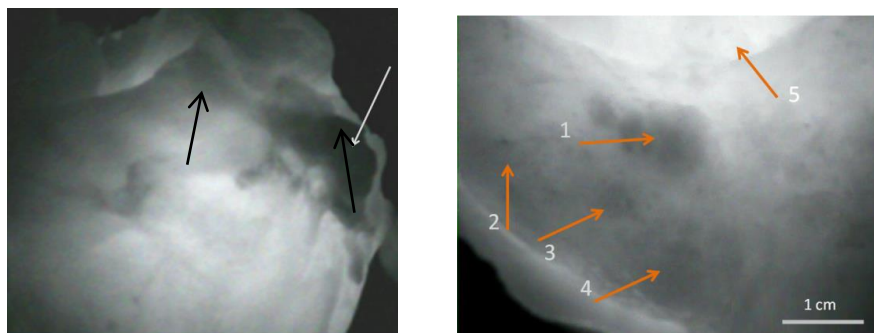


*Figure 28. On the left-The cancerous prostate IR image. With black arrows we can see cancerous tissues with Gleason score 6. With white arrow we can see malignant tissue with Gleason score 8. On the right- IR image the other cancerous prostate. The cancerous tissues are diffused through prostate assmall size acini, shown with arrows 1-4 . We can see that, these acini are few mm in size (compare with 1 cm scale.) With 5<sup>th</sup> arrow we can see high intensity area, which is because thin thickness and so more light passes through prostate tissue.*

Experiments showed that the more aggressive is cancer, the darker is its IR image and vice verse. On the figure 29 is shown histomorphological expression of the same prostate tissue.

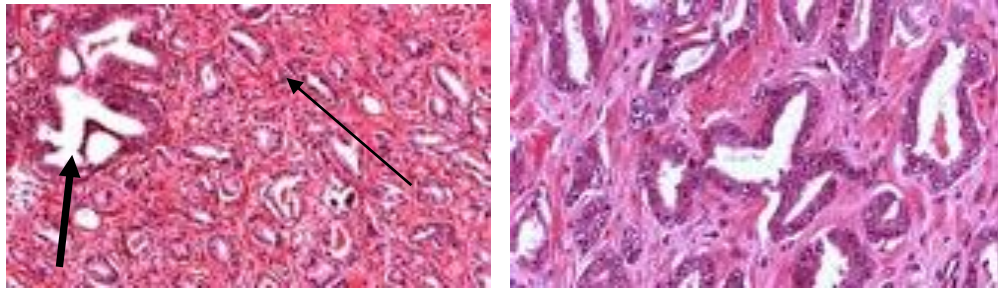


*Figure 29. The cancerous prostate histo-morphology pictures. On the left figure is shown histo-morphological image of prostate tissue, which was shown in the figure 28 –left hand side. Gleason score in this case was 8 (4+4). On the right we see histo-morphological image of prostate tissue with Gleason score 5. This prostate is on the right side in the figure 28.*

Arised question - does formalin effects on formation of the prostate IR image? On the figure 30 one of the prostate treated in formalin and its IR image are shown.

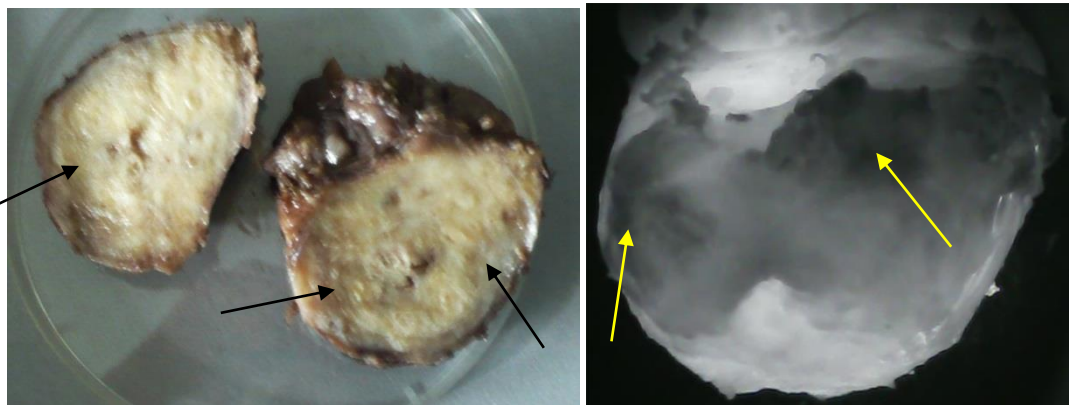


*Figure 30. On the left photography of the prostate treated in formalin. The prostate was cut and malignant tissue is shown with arrows. On the right we see IR image of this prostate. The cancerous formations are shown with arrows.*

Experiments revealed, that formalin doesn't prevent on the IR image formation. So we can freely use it, to get IR images later.

In real situation IR light passes through rectal wall and its fatty tissues before entering into the prostate. For this purpose we performed model experiments. On figure 31 we see results of this experiment.

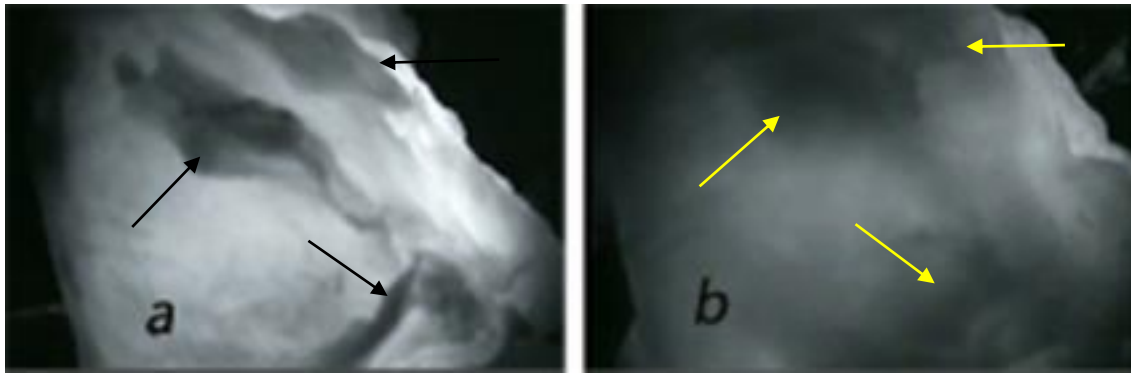


*Figure 31. On the left we see cancerous prostate IR image. The cancerous areas, as in other cases, are seen like dark areas (shown with arrows) on light background. Then the same prostate was covered with rectal tissue (the tissue was taken from the pig's rectum). On the right figure we see IR image of the same prostate covered with rectum tissue. It is easy notable that all cancerous areas are retained in this case -which are shown with arrows.*

Thus, in real situation rectal wall doesn't have any influence on IR image formation.

From literature is known, that in 80 % cases prostate cancer arises at peripheral zone, which is between urethral channel and and rectum wall. This is the reason why we plan to place IR light source in prostatic part of urethra in future. We performed investigations during which IR light source was placed in urethral channel. The placement of light source in urethral channel enables us to make more accurate IR image. On figure 32 we see cancerous prostate IR images, which are taken by this method.

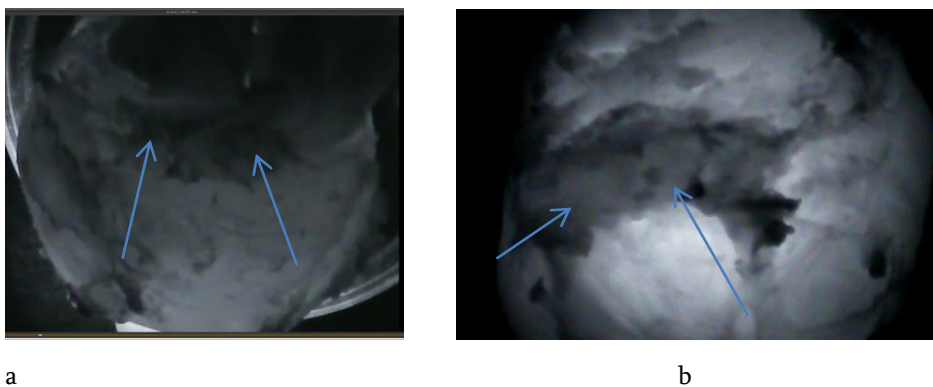
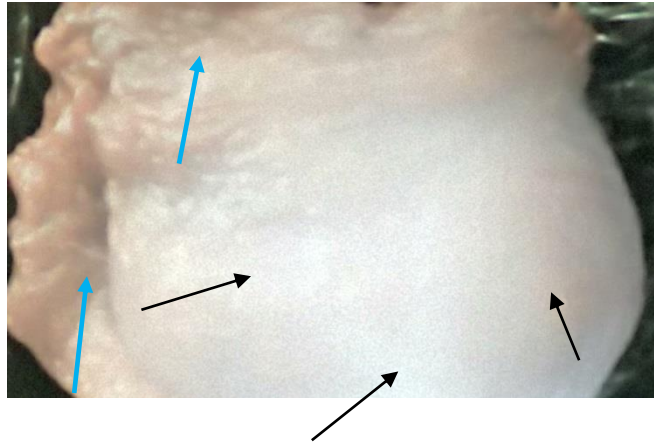


*Figure 32. Cancerous prostate IR images. On the left image is taken via placement of LED outside of the prostate, on the right -LED was placed in urethral channel. Malignant areas are shown with arrows.*

Thus, the experiments showed that, illumination of the prostate from the urethral channel gives images with better quality.



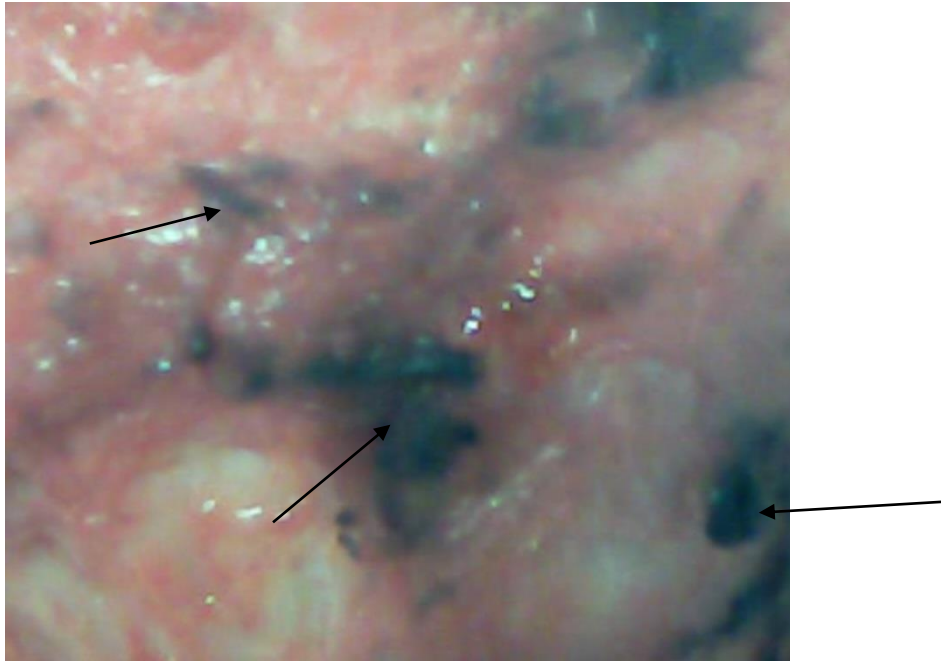
Task conceived investigation of prostate IR images in back scattered IR light. In this case prostate IR illumination can be performed by placing light source and CCD camera together. On figure 33 is shown one of prostate IR image taken using these techniques.



*Figure 33. Nonmalignant prostate IR image taken with back scattered light. Penetration of IR light in the prostate tissue is different in different places. Light blue arrows shows reflected IR light from the prostate surface. The black arrows show back scattered light from the deeper layers of the prostate .*

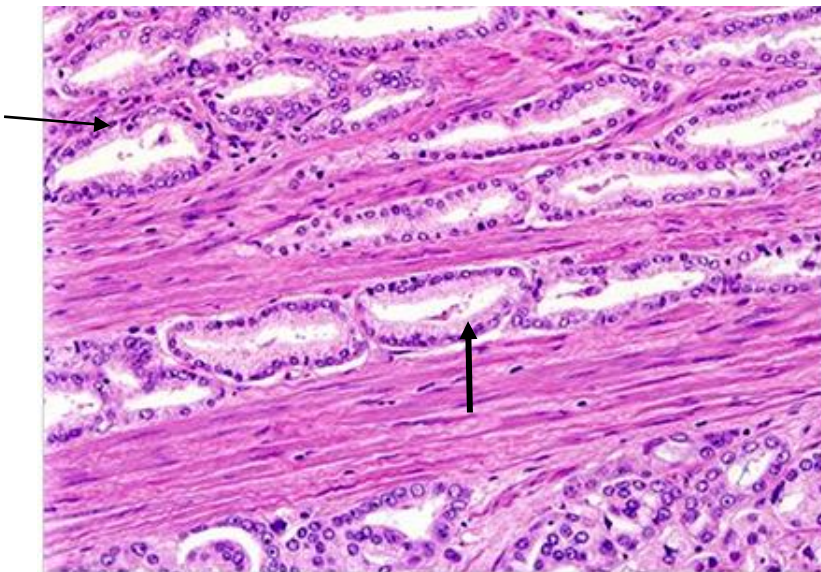
Results shown on the figure 33 can be explained as follows: prostate areas showing with the light blue arrows have less thickness, then areas shown with black arrows. Areas shown with light blue arrows are fully transparent to IR lights, that's why reverse lightning doesn't happen. The areas shown with black arrows have more thickness, that's why: the part of light is reflected from the prostate surface and part transmits prostate tissue; The part of light is passed through prostate and part of light is reflected back and detected by CCD camera.

Experiments showed that, areas which have same thickness have same brightness. Experiments have shown that transmitted lights and reflected lights of cancerous and noncancerous prostate images are different from each other. Figure 34 shows prostate IR image with reverse lighting.



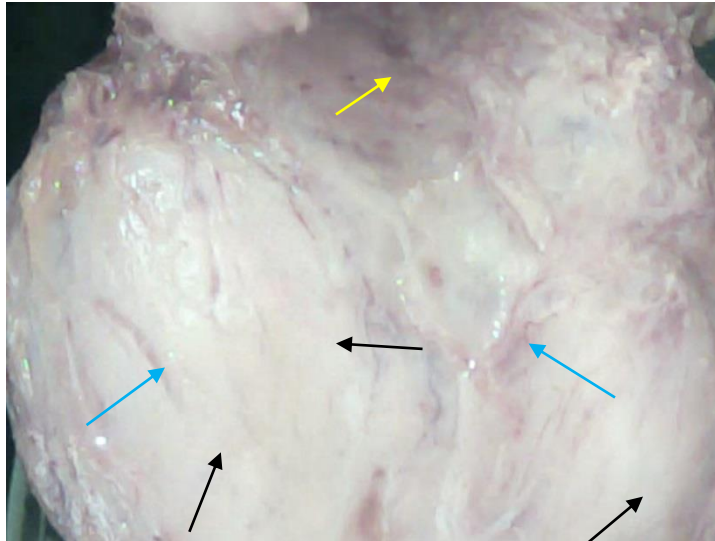
*Figure 34. Cancerous prostate IR image with reverse light, arrows show malignant areas*

The histo-morphology of this prostate showed that this cancer has Gleason score 7- Figure 35.



*Figure 35. Prostate normal acines placed in different areas with thin arrow, malignant acines are in fibromuscular stroma-thick arrow.*

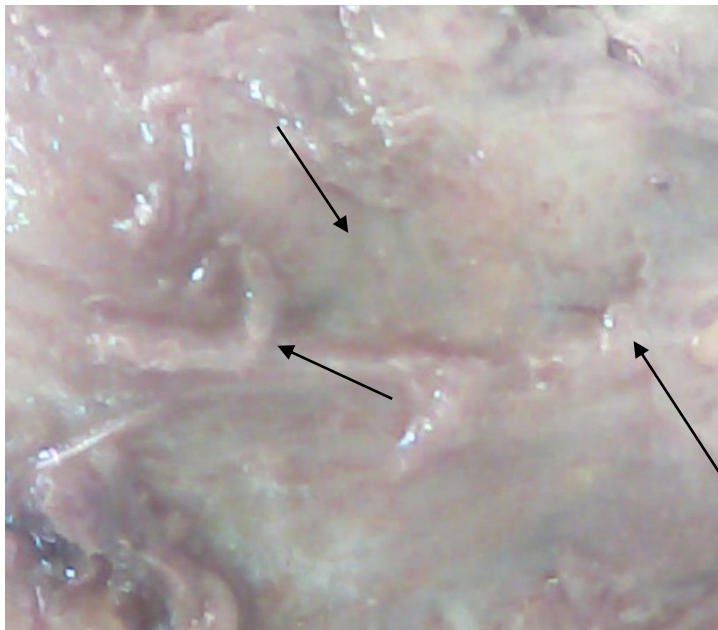
Experiments showed that: 1) if cancerous tissue is close to prostate surface can be detected with back scattered light. 2) If cancerous tissue is located in deeper layers its detection is not possible. This is shown on figure 36.



*Figure 36. Cancerous prostate IR image taken with back scattered light. Difference between areas indicated with black and light blue arrows is not seen.*

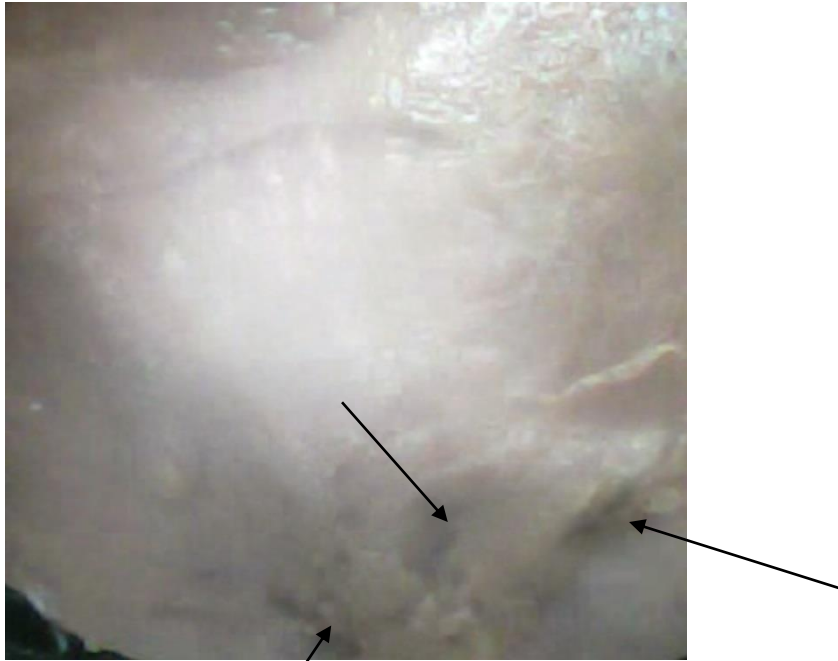
Histo-morphology investigation showed that cancerous tissue was at the area shown with yellow arrow. This cancerous formation was close to surface. At the areas shown with black arrow cancerous outgrowths were located in 2-3 cm depth in the gland. Here Gleason score was 6. Areas shown with light blue arrows are of unclear origin. Malignant areas which are in deeper structures could not be detected even in case of higher Gleason score.

Figure 37 shows cancerous prostate IR image with back scattered light where Gleason score was 8. The cancerous area was in the depth of urethral channel, unfortunately reverse lights could not detect it.



*Figure 37. Cancerous prostate IR image with reversed rays. Arrows shows nonhomogeneity of prostate surface.*

We wondered what was the reason of detection difficulty and could it be conditioned by the water composition of prostate tissue. To answer this question we have done experiments with formalin prepared prostate. It is known that formalin removes water. Result of one of these experiments is shown on figure 38.



*Figure 38. Formalin prepared prostate IR images taken with reverse rays. Arrows show suspected places. IR images have non homogenous appearance. On the right side below high optical density areas are seen.*

Histo-morphology investigation showed that high optical density areas corresponded to cancerous outgrowths with the Gleason score 6, but similar aggressiveness areas were found in 3 cm depth at the center, which is not detected by IR image. In conclusion: the role of water in detection difficulty is excluded. So experiments showed that reverse light rays are not informative in prostate cancer detection.

The project conceived prostate IR investigation with polarized light. The figure 39 compares images taken with non polarized and polarized IR lights.



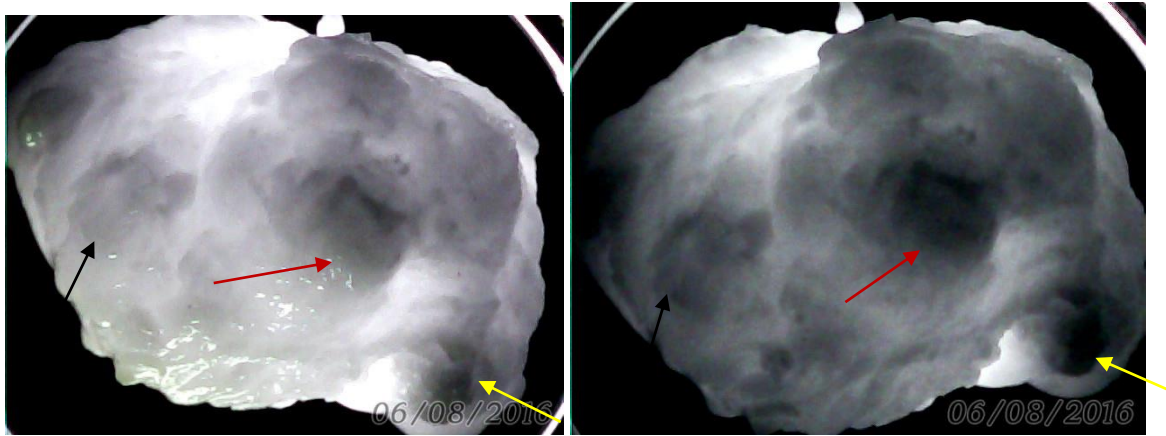


*Figure 39. One and the same prostate IR images. On the left figure IR LED is placed outside of the prostate. The image is taken by non polarized irradiation. On the right side the same prostate IR image taken with polarized light. The malignant areas are shown with same color arrows.*

To get polarized images polarizing films are placed: One between LED and prostate, the second before the CCD camera, above the prostate. Film polarization E vectors are perpendicular to each other. If no objects are placed between polarizing films, intensity will be equal to zero in CCD camera. If prostate is placed between polarizing films, polarized light passes through prostate tissue. Polarization angles turns and image is seen. The LED is same in both cases, the same is intensity of the IR lights. It was noted that, image taken with polarized light has less brightness. This is caused because in polarizer pass only part of light rays. A polarized light enables us to see more cancerous structures.

As experiments showed, malignant tissue have dark appearance on light background. The light background corresponds to nonmalignant prostate tissue. That's reason why noncancerous prostate image brightness is homologous. Cancerous (malignant) tissue's optical density in IR region is much higher than of normal tissue. To conclude that: figure 40 shows prostate cancerous cell scheme with different pattern of aggressiveness.

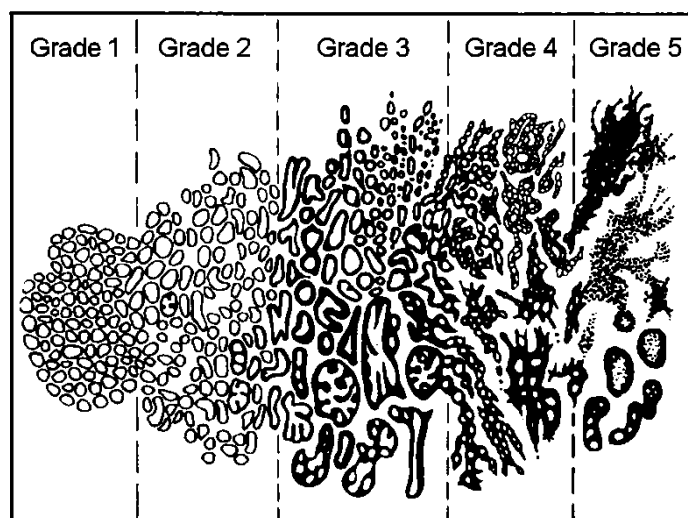


*Figure 40. (From literature). The prostate cancer cell scheme, which have Gleason score from 5-10 ( Grades 1-5). As the Gleason score gets higher cells get unusual forms, image gets darker and cells do not pass light.*

Cancer cells differ from normal cell in microscope (visible light), this difference is following: normal cells have one nucleus and nucleolus, in cancer cells nucleus and nucleolus are more than one, also they have different division pattern. Because of their structure, more aggressive cancer cells are less transparent to the light, then normal ones. The logic is same in case of infrared spectrum too (invisible to human eye), high optical density cancerous cells are less transparent than normal ones.

It is obvious that brightness intensity perception is subjective. To overcome this computer program was developed for prostate cancer detection.

Information about different intensity coming from CCD camera software divides in 256 different brightness patterns. Zero level is for “dark” image- this refers to situation where IR lights are fully absorbed by prostate tissue and do not enter CCD camera. Level 255 is for situation, where prostate is fully transparent for IR light, which enters CCD camera. When IR image is analyzed software gives specific code to suspicious areas. The same happens for normal tissue, which will get another code. On the figure 41 we see computer image gathered so and areas labeled by this method.

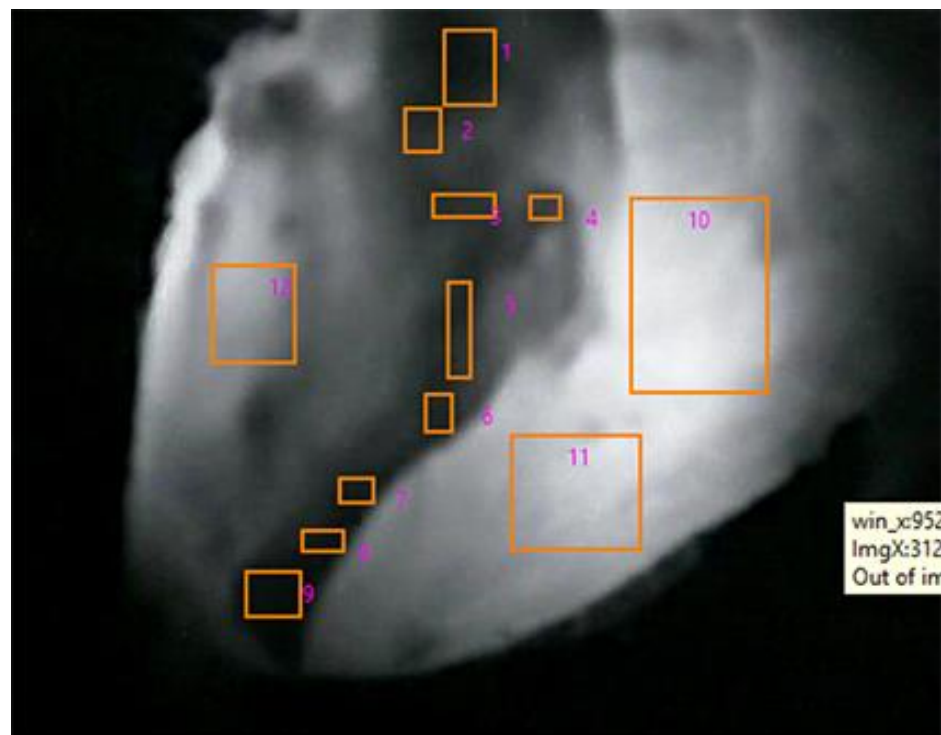
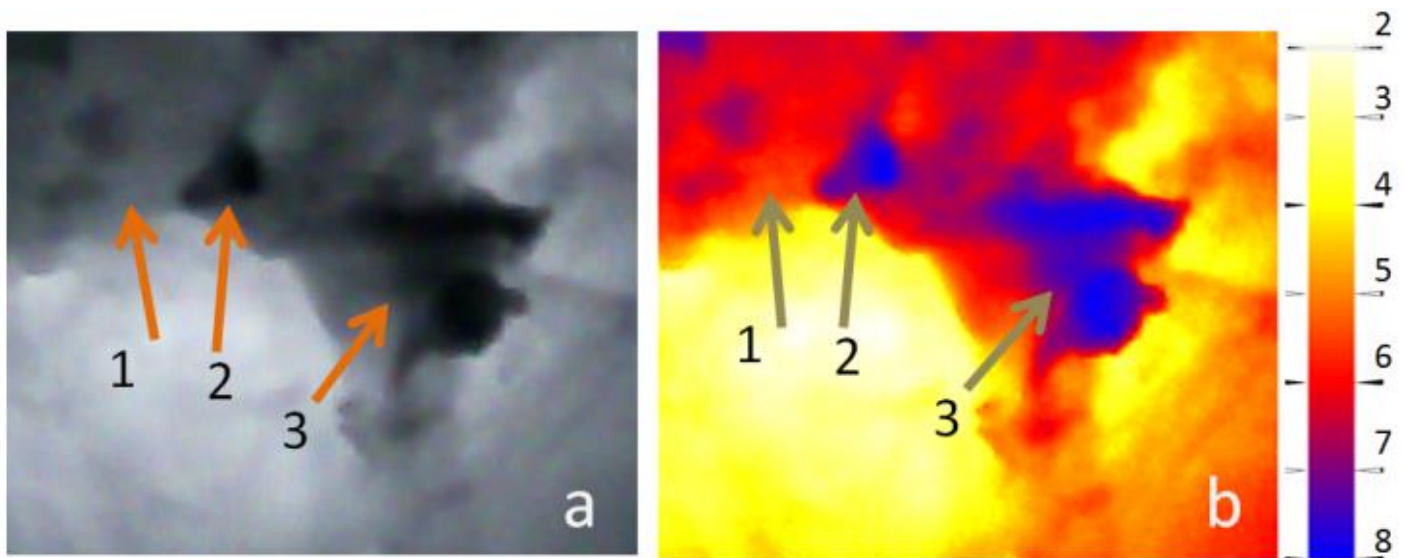


Figure 41. Cancerous prostate IR image . Labels 1-9 are for malignancy. Labels 10-12 –for normal tissue.

After this program will automatically calculate labeled area brightness intensities and their mid meaning. The same happens for normal tissue. Software then calculates their ratio. The following procedure is done for

every other prostate, after those in program memory will be gathered sequence of numbers. These numbers represent intensity ratio values for all experiments. The software calculates so called “95 % confidence interval”. If the next prostate with unknown diagnosis will be examined with IR method, program will calculate it's intensity ratio and compares obtained number with calculated 95% confident interval. If calculated number will occur (falls) in the mentioned 95% interval, we can declare with 95% probability that this new prostate is cancerous. Specially should be noted that histo-morphology results completely confirmed software results. The software has another ability also -color service. In detail, software gives different colors to areas with different aggressiveness of cancer, which is shown on figure 42.



*Figure 42. Fragment of cancerous prostate in grayscale (on the left) and color representation (on the right). Arrow 1 shows malignant area with Gleason scores 5 on both figures. Arrows 2 and 3 show malignant areas with Gleason scores 8. On the right side, there is bar, where blue color corresponds to the Gleason score 8, red- to the 6, yellow- to the 4 and white-normal tissue.*

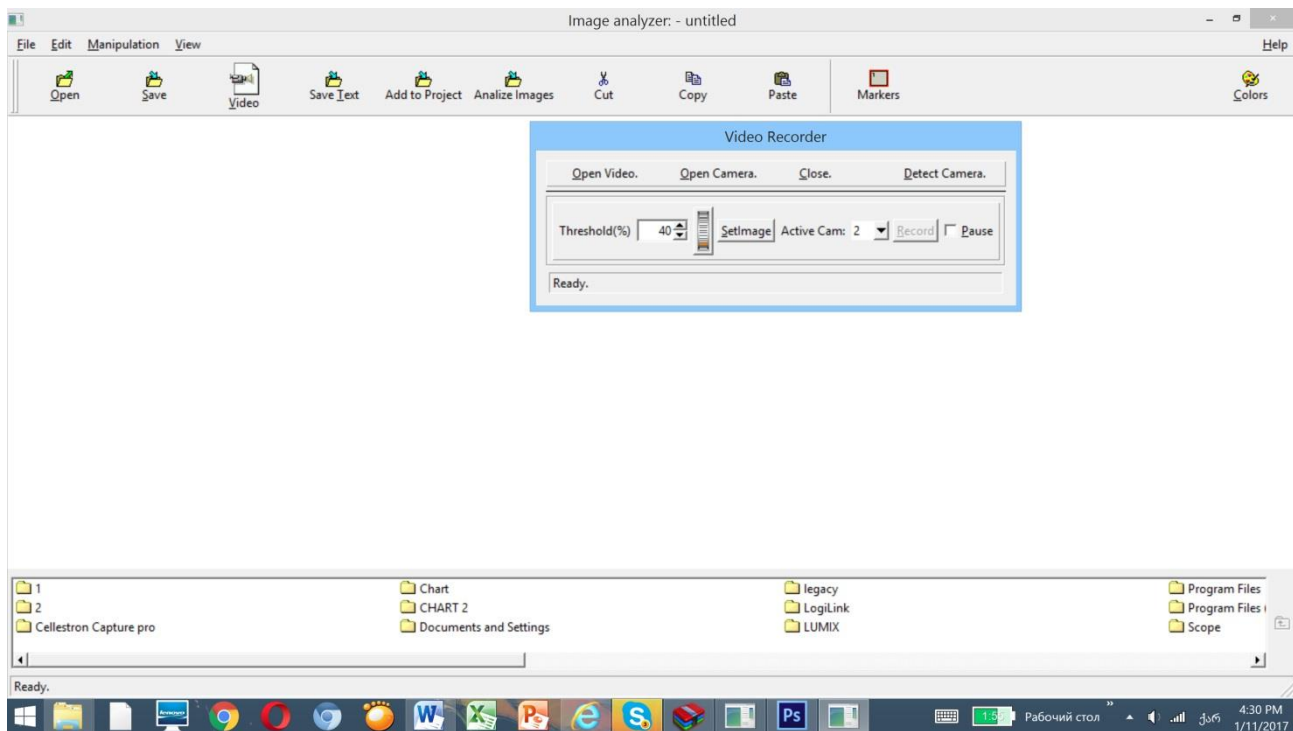
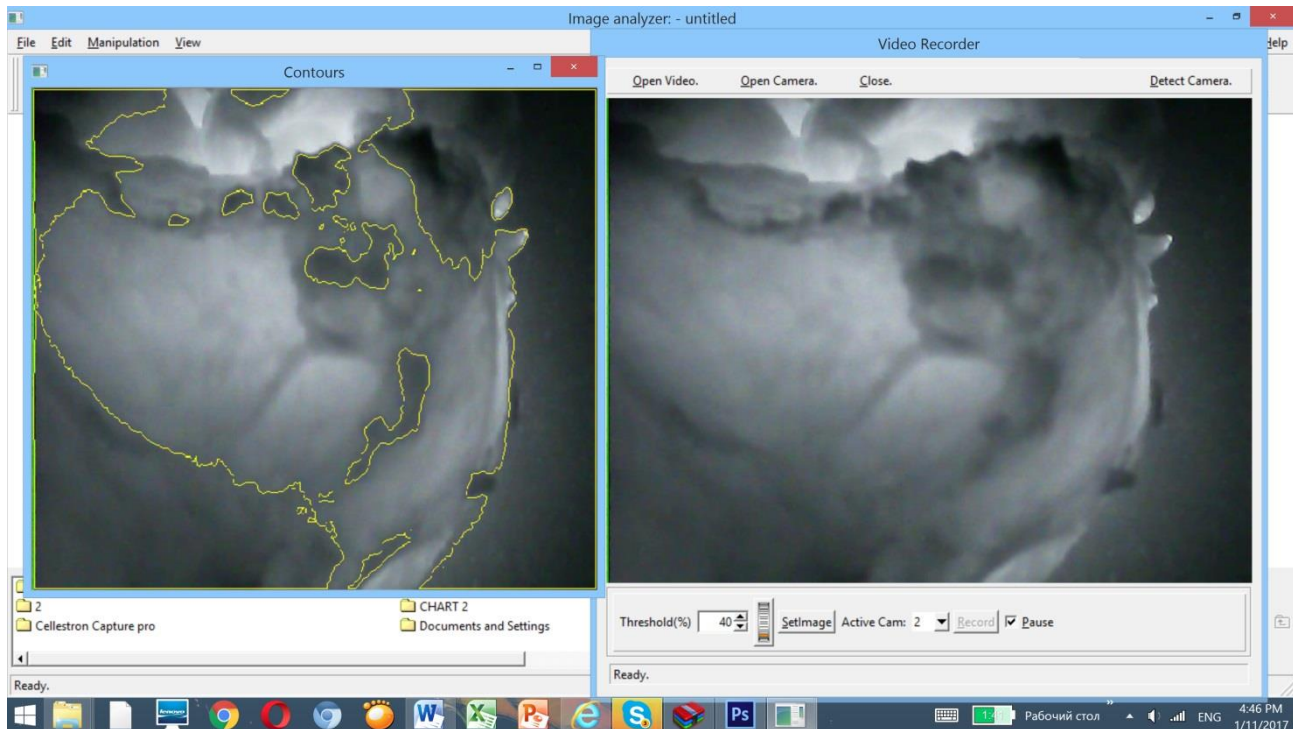


figure 43. Software (program) interface image.

The program has different options. It enables us to get and edit IR images, during live or offline mode. For these are “open camera” or “open video”.

Program has ability to iscriminate high density areas from less density ones. The program encircles those areas. Figure 44 shows cancerous areas labeled by the software.





*Figure 44. Software during working process. On the right side software is in “live “ mode. On the left side high optical density areas devided from low optical density ones.*

In case of urinary cancer, the urinary bladder and prostate are both taken out, with/without prostate malignancy. The IR diagnosis are made for those prostates too. Figure 45 shows this kind of prostate and its IR image. The prostate was not mentioned as malignant, as patient PSA was equal to 2,4.

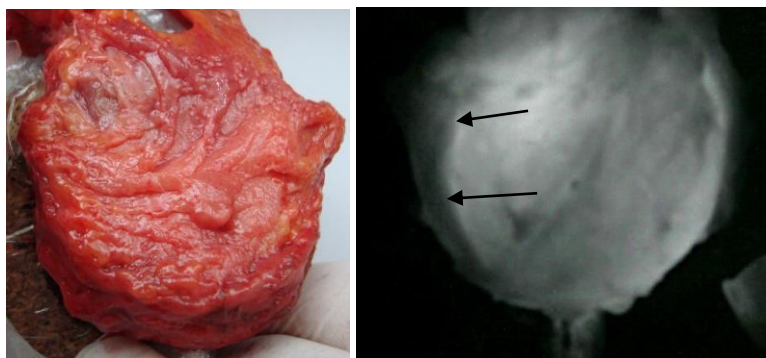


*Figure 45. On the left –prostate photography, on the right –its IR image. Here on the left side of prostate we found high density areas-shown with arrows.*

After IR investigation high optical density areas was found on the left side. The histo-morphology was needed, after which prostate acinar and smallacinar carcinoma, with Gleason score 6 (G's 6 (3+3)) was detected. Histo-morphology confirmed the diagnosis of infra red investigations.

As it is known, for every prostate histo-morphology examination slices must be made and then placed on special cassettes. Their numbers are few tenths. After slice preparation everything must be examined under the microscope. This is hard work and time consuming task. Our results can diminish number of cassettes and slices, also time which was used to examine them. The IR light enables us to label precisely malignant areas, so it can help us in histo-morphology examination too.

On the basis of our experiments we developed and fabricated working prototype of device for prostate cancer visualization and diagnosis. Developed device consist from: IR light sensitive part, lightening system, computer program and computer.

We have fabricated two versions of above mentioned device. One of them is shown on the figure 46.



*Figure 46. Photography of prostate cancer diagnosis device. Yellow arrow shows the window, under which CCD camera matrix and lens system are placed. With the red arrow is show camera end, which is connected to computer.*

*Device sizes: diameter 19mm, length 170 mm.*

The focal distance of the lens system is 7 mm. Active area of the device is 10mm x 10mm.

For the second sample form was taken from “digital rectal examination” method. We tried to give the device curved finger form. Here lens system focus length is 25 mm. Active area of the device is 2cm x 2cm.

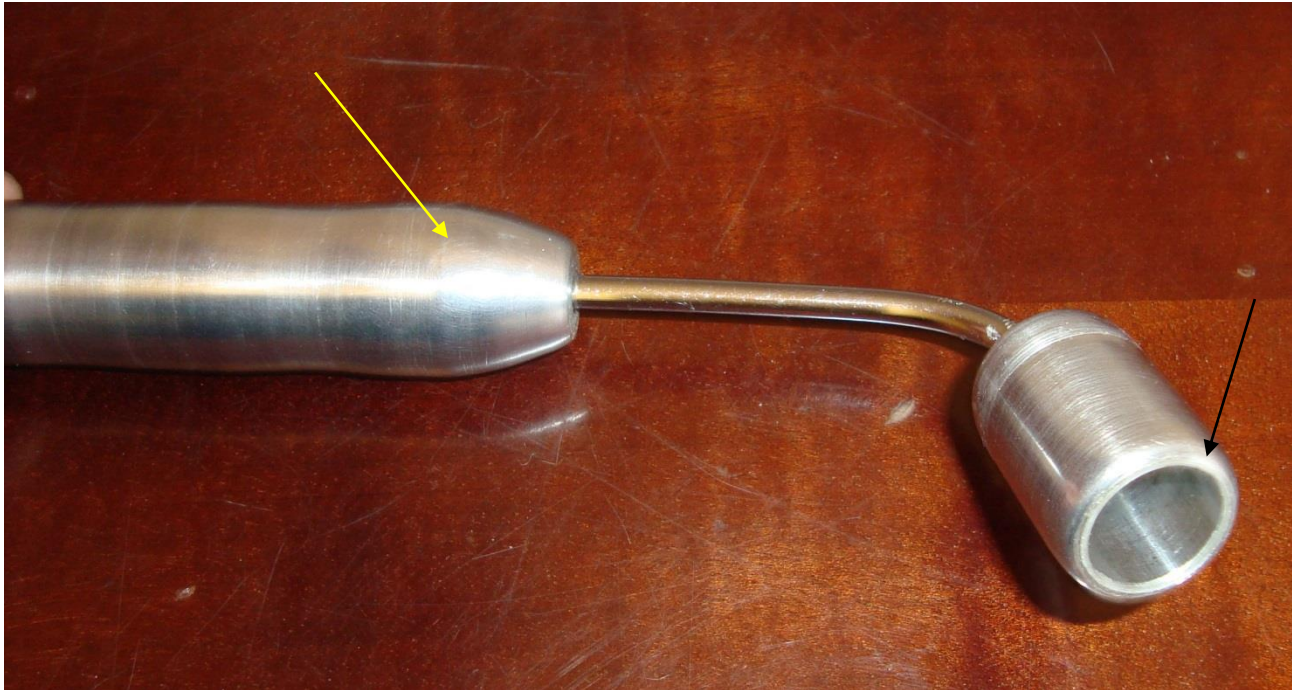


*Figure 47. Prostate cancer diagnosis device. Black arrow shows the head where CCD matrix and lens system are placed. With yellow arrow is shown the handle.*

The device sizes are: diameter of head-23mm, handle length-33mm. The dimensions are a little bit more than average finger size of human. Handle sizes are- length-10cm, diameter -2, 4 cm. In future we are planning to examine these samples on patients and their forms will be better modified later.

Light sources: In the first case, when prostate should be lighted from urethral canal, we have made mini sized lighter. It will be placed in sterile catheter, which will enter in prostatic urethra. The catheter has single use only. Lighter sizes: diameter-1, 4mm, length-20mm. Energy source is with CD-voltage 9V. Outer diameter of catheter is not above 3,5 mm.



Figure 48 shows lighter , which irradiates IR light.



*Figure 48. Urethral canal lighter device, composed of IR LEDs.*

In the second scenario, when IR lighter should be placed above the patient abdomen. IR rays source is seen on the figure 49.



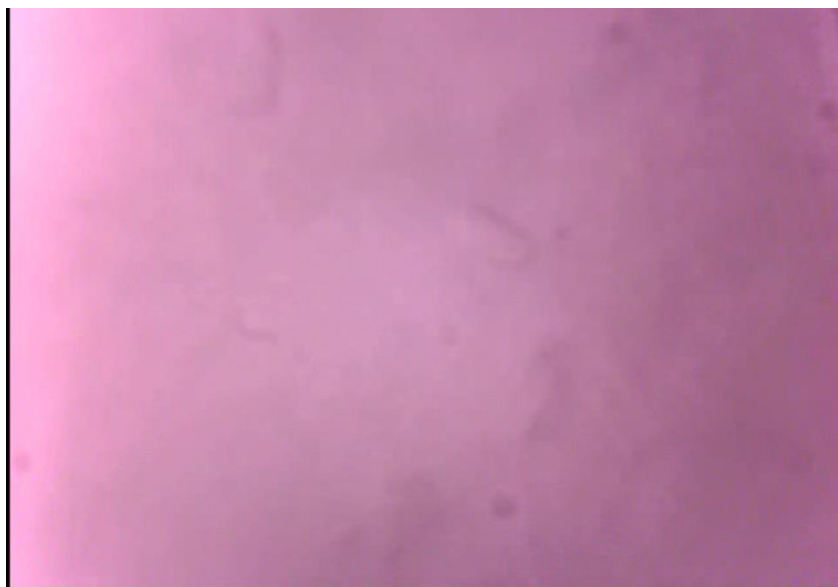
*Figure 49. 60 watt power IR lighter.*

Experimental series were performed using these two diagnostic devices. Figure 50 sows one of the devices and prostate.



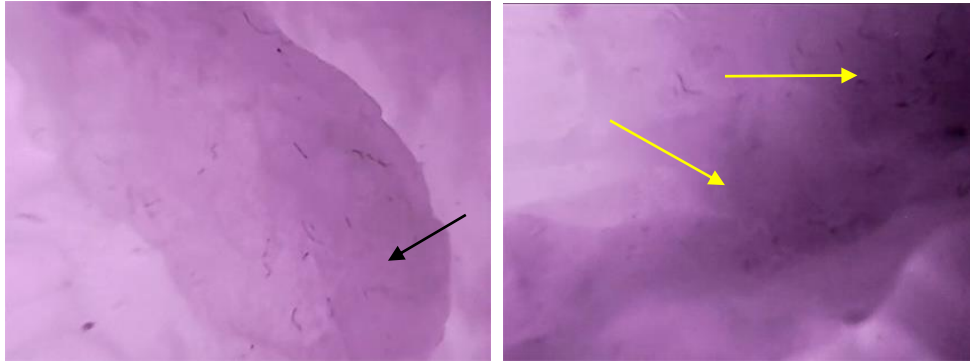
*Figure 50. Device (shown with the arrow) and prostate.*

Figure 51 shows IR image of nonmalignant prostate obtained using this device.



*Figure 51. IR image of nonmalignant prostate obtained using the device. Image brightness intensity is homogenous, because it has not malignant areas.*

Figure 52 shows IR image of prostate cancer detected by the device in the case of cancerous prostate.



*Figure 52. Fragments cancerous prostate IR images detected by new device. The arrow shows high optical density areas, which corresponds to cancerous outgrowths.*

Following histomorphology showed that o these areas correspond Gleason score 6 - left, and Gleason score 8 - right.

Figure 53 shows malignant areas detected by the second device, which is shown in the figure 47.

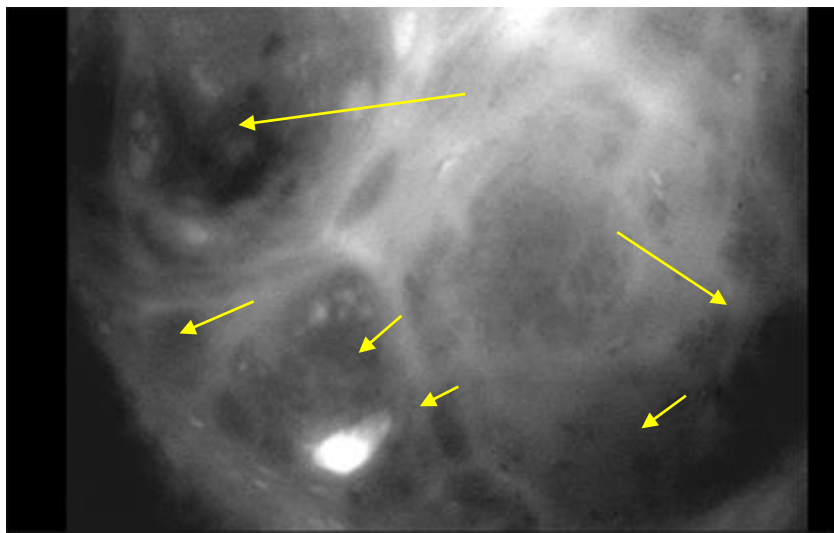


*Figure 53. cancerous areas are shown with the arrows, which are detected by the second device.*

Given device has lens system with a little bit long focus distance, which enables us to see the more surface area of the prostate. Next histo-morphology showed that areas shown with arrows had aggressiveness with Gleason scores 6 and 8.



## 4. Conclusion

### Findings:

- Prostate tissue is transparent to IR rays and max. transmittance is detected at 840-860 nm wavelength.
- Nonmalignant prostate tissue is more transparent, then malignant one.
- Transmitted rays intensity can be regulated by changing lighter intensities.
- Normal and BPH prostate tissues transmitted IR rays intensity is inversely proportional to prostate thickness. This dependence is linear.
- Malignant prostate tissue transparency for IR light is nonlinear.
- Nonmalignant prostate IR image's brightness is homogenous.
- Cancerous prostate brightness is non-homogenous. Cancerous areas have high optical density in IR images.
- The Cancerous areas density depends on their aggressiveness of the tumor. As higher is aggressiveness as higher is optical density.
- Reverse light rays are not useful for prostate cancer diagnosis and visualization.
- The preparation of prostate in formalin does not prevent formation of IR images.
- Developed software (computer program) enables us to get and work prostate IR images in online and offline modes.
- The software calculates confidence interval and enables us diagnose unknown prostate and its risk of malignancy with accuracy of 95%.
- The prostate cancer diagnostic devices are made to examine different prostates.
- The device enables us to detect small sized cancerous areas.

## 5. References

Attachment 1: List of published papers and reports with abstracts

Attachment 2: List of presentations at conferences and meetings with abstracts